Geoderma 232–234 (2014) 600–608

Contents lists available at ScienceDirect

Geoderma

journal homepage: www.elsevier.com/locate/geoderma

Adsorption and surface precipitation of phosphate onto $CaCO_3$–montmorillonite: effect of pH, ionic strength and competition with humic acid

Ileana Perassi [a], Laura Borgnino [b,c,*]

[a] Facultad de Ciencias Químicas, Universidad Nacional de Córdoba, Ciudad Universitaria, 5000 Córdoba, Argentina
[b] Centro de Investigaciones en Ciencias de la Tierra (CICTERRA), Instituto de Investigaciones en Físico-Química Córdoba (INFIQC), Universidad Nacional de Córdoba, Ciudad Universitaria, 5000 Córdoba, Argentina
[c] Departamento de Fisicoquímica, Facultad de Ciencias Químicas, Universidad Nacional de Córdoba, Ciudad Universitaria, 5000 Córdoba, Argentina

ARTICLE INFO

Article history:
Received 5 February 2014
Received in revised form 15 May 2014
Accepted 17 June 2014
Available online xxxx

Keywords:
Phosphate adsorption
Calcite-montmorillonite
Competition
Humic acid
Raman spectroscopy

ABSTRACT

The adsorption of phosphate onto $CaCO_3$–montmorillonite (calcite–M) was studied in a series of batch experiments and in a wide range of phosphate concentration (5–160 μM). Our results show that phosphate adsorption is dependent on pH; adsorption increases as pH decreases. Phosphate initial concentration and ionic strength also affects the process of phosphate removal, prevailing adsorption for phosphate concentration lower than 100 μM, while surface precipitation of HAP and carbonate apatite is favored at high phosphate concentration and ionic strength. Raman spectroscopy shows both the transition between adsorption and surface precipitation and the Ca–P compound formed.

The presence of a competitor, such as humic acid, reduces phosphate adsorption and reveals that both ions are in competition for surface sites. Depending on the order that the adsorbates are added, higher reduction occurs when humic acid is added first. In contrast, when phosphate is added first, the adsorption increases significantly with respect to the values obtained in the absence of humic acid. Humic acid may prevent precipitation of Ca–P compounds, leaving more phosphate available in solution to be adsorbed.

1. Introduction

The availability of phosphates for plant uptake is an important agricultural issue, especially in arid and semi-arid regions with calcareous soils. Phosphorous is an essential plant nutrient and low level of phosphate can limit production. During the past few decades, low availability has been amended with the addition of phosphate in the form of manures and fertilizers. However, in most calcareous soils, it was found that the addition of fertilizers did not produce any agronomic advantage, as productivity in some of these areas did not increase (Castro and Torrent, 1995; Delgado et al., 2000; Sample et al., 1980; Wandruszka, 2006). As a consequence, the over-application of the nutrient has led to the eutrophication of natural reservoirs, which in turns, leading to a degradation of water quality.

Once phosphate is added to calcareous soils, a series of reactions that gradually decrease its availability to plants can occur. The main reactions involved are adsorption onto calcite, Fe(hydr)oxides, clay minerals, and precipitation of phosphate as calcium phosphate minerals (Cole et al., 1953; Delgado et al., 2000; Freeman and Rowell, 1981; Liu et al., 2012; Yagi and Fukushi, 2012). A general consensus has affirmed that phosphate can be either adsorbed by calcite at low concentration or precipitated at high concentration (Freeman and Rowell, 1981; House and Donaldson, 1986; Klelner, 1988; Liu et al., 2012; Yagi and Fukushi, 2012), although it is not always easy to distinguish between these two mechanisms. Early works (Cole et al., 1953; Stumm and Leckie, 1970) suggested that the initial uptake of phosphate onto calcite occurs via chemisorption, which is then followed by a slow transformation of amorphous calcium phosphate to crystalline apatite. The adsorption can be described by Langmuir adsorption isotherms (Karageorgiou et al., 2007; Millero et al., 2001; Sø et al., 2011; Yagi and Fukushi, 2012) and can take place on a limited number of sites when phosphate concentrations is low. At high concentrations, the process starts with small amounts of phosphate adsorption, followed by the precipitation of Ca-compounds, such as dicalcium, brushite, octacalcium phosphate and hydroxyapatite (Freeman and Rowell, 1981; Yagi and Fukushi, 2012).

As well as calcite, clay minerals can adsorb phosphate. Despite the large surface area that clay minerals have, research has proven that phosphate adsorption onto clays is very poor (Borgnino et al., 2009; Yin et al., 2011). The high net negative charge that clays minerals have (e.g.: montmorillonite) prevents interaction with phosphate. Clay minerals, therefore, are not good adsorbents for phosphate removal.

* Corresponding author at:Centro de Investigaciones en Ciencias de la Tierra (CICTERRA), 5000 Córdoba.
E-mail address: borgnino@fcq.unc.edu.ar (L. Borgnino).

http://dx.doi.org/10.1016/j.geoderma.2014.06.017
0016-7061/

In addition, phosphate dynamics in calcareous soils are also dependent on the organic matter. There is evidence that organic matter may increase the availability of phosphate (Delgado et al., 2002; Staunton and Leprince, 1996; Violante and Gianfreda, 1993), due to the competition of both anions for the same adsorption sites. Furthermore, organic compounds can also affect the rate and manner in which phosphate precipitates, such as inhibiting the formation of hydroxyapatite (HAP) (Alvarez et al., 2004; Delgado et al., 2002; Grossl and Inskeep, 1991; Inskeep and Silvertooth, 1988; Oelkers et al., 2011). Both effects are beneficial, as more phosphate would be available to plants, improving soil productivity.

Although several studies have been focused on the adsorption of phosphate onto calcite, literature shows differing results in regards to this question, especially on the effect of pH and ionic strength on phosphate adsorption. Liu et al. (2012) found that phosphate adsorption decreases from acidic pH to neutral-alkaline, reaching a minimum of adsorption at pH 10.0, and then increased with pH. In opposition to this finding are the results of Karageorgiou et al. (2007) and Millero et al. (2001), which observed an increase in the phosphate adsorption as pH increased. The effect of ionic strength was less evaluated. Sø et al. (2011) and Yagi and Fukushi (2012) explained that an increased in ionic strength produced an increase in the concentration of negatively charged surface species, so the adsorption of phosphate is reduced. Millero et al. (2001) found similar results, but attributed this effect to the concentration of HCO_3^- in the waters, that competes with phosphate to the same surface sites. In regards to the effect of organic matter on the phosphate adsorption, a general agreement indicates that its presence increases the phosphate available (Alvarez et al., 2004; Delgado et al., 2000, 2002; Grossl and Inskeep, 1991; Inskeep and Silvertooth, 1988; Oelkers et al., 2011). However, the effect of the order of addition of adsorbents on the adsorption of phosphate remains limited.

In addition to the above differences observed, all of these experiences were made using calcite as an adsorbent. However, in natural environments (such as calcareous soils) phosphate is not only adsorbed onto pure calcite, but also in calcite coatings (e.g.: calcite-coating phyllosilicates). It is expected that the surface properties of calcite differs from calcite-coating phyllosilicates, and therefore the phosphate adsorption capacity also changes. Very few studies have been carried out on the adsorption behavior of phosphate on calcite-coating phyllosilicates (Violante and Gianfreda, 1993; Yin et al., 2011) and the competitive adsorption effect of humic acid on phosphate adsorption (Delgado et al., 2000, 2002).

This study primarily aims to investigate the adsorption of phosphate onto calcite–M ($CaCO_3$–montmorillonite) and to analyze the competitive effect between humic acid and phosphate for calcite–M surface sites. Adsorption isotherms were evaluated under different pH and ionic strength conditions. By analyzing the solubility curves in combination with results obtained from Raman spectroscopy, the conditions of pH and ionic strength that favor the adsorption process or surface precipitation were evaluated. The view offered by Raman spectroscopy measurements is complemented here by macroscopic data, such as adsorption isotherms and solubility curves. For the competition study, a series of experiments was carried out to assess the effects of both the addition of humic acid, and also the order of addition of adsorbates on the phosphate adsorption.

2. Materials and methods

All solutions were prepared from analytical reagent grade chemicals and purified water (Milli-Q system).

2.1. Synthesis of Na and $CaCO_3$–montmorillonite

The montmorillonite used in this study was obtained from Cerro Banderita (Province of Neuquén, Argentina). Particles with a diameter of <2 μm were obtained by sedimentation and saturated with Na^+ by treating the clay suspension with 1 M NaCl. The sodium exchanged clay (Na–M) has a cation exchange capacity of 91.7 meq/100 g (Peinemann et al., 1972).

For the synthesis of the $CaCO_3$-montmorillonite, a weighed amount of solid $CaCl_2 \times 2H_2O$ was dissolved in water to obtain a 0.05 M of Ca(II) solution; its pH was adjusted to 3.5 with HCl. Then, this solution was mixed with 250 mL of a 4.0% Na–M dispersion in water, whose pH had previously been adjusted to 3.5. After 2 h of vigorous magnetic stirring at this pH, a certain amount of Na_2CO_3 solution (0.05 M and pH 11.4) was added. The final pH of the mixture was 8.8. Under these conditions, the dispersion was stirred for 45 min and then was left to age for 20 h. After that, the solid was washed with water and dried at 60 °C. This sample referred to herein as calcite–M.

2.2. Characterization methods

Chemical analysis of the Na and calcite–M was carried out by ICP/OES after lithium metaborate/tetraborate fusion. The specific surface area (SSA) for both samples was measured by N_2 adsorption using a computer-controlled STROHLEIN area meter II instrument.

In order to characterize the presence of the calcite in montmorillonite sample, Powder X-ray diffraction (XRD) was conducted on both samples (Na–M and calcite–M). XRD patterns were recorded with a Philips X'Pert PRO X-ray diffractometer, using CuK_α radiation (30 kV–15 mA). XRD data was obtained in the 2θ range from 4 to 70° (step size: 0.01; 6 seg/step). The reflection assignments were completed using the X'Pert HighScore software, installed on the X-ray diffractometer.

The zeta potential measurements were carried out using the Delsa Nano Size (Beckman) apparatus. Na–M and calcite–M suspensions (0.5 g L^{-1}) were prepared by dispersing the samples in 0.01 M of $NaNO_3$. The suspension pH was raised to approximately 3.5 with HCl, and the zeta potential measurement was carried out. After that, the pH was slightly increased with NaOH and a new measurement was performed. This procedure was continued until the pH reached approximately 9.0.

2.3. Sorption experiments

The adsorption experiments were carried out by batch method. Appropriate stock solutions of phosphate were prepared by dissolving respectively sodium phosphate ($Na_2HPO_4 \times 7H_2O$) in water. Determined amounts of calcite–M (1 g L^{-1}) were suspended in 0.1, 0.01 and 0.001 M $NaNO_3$ solution as background electrolyte in 50-mL polyethylene centrifuge tubes precleaned with 1% HNO_3 and several times with deionized water. After 24 h pre-equilibration, a well-known volume of a 0.01 M phosphate solution ($Na_2HPO_4 \times 7H_2O$) prepared in the same electrolyte concentration of $NaNO_3$ was added. The phosphate initial concentration range was thus 5–160 μM. This range of concentration was selected in order to assess both adsorption as well as the formation of calcium–phosphate compounds (Ca–P compounds) at high phosphate concentrations. After that, the pH of the suspension was adjusted by the addition of a small amount either HNO_3 or NaOH, until the desired pH was obtained (pH values 4.5, 7.0 and 9.0). Based on preliminary kinetic experiments, the equilibration time was set to 3 h for all adsorption experiments (see Fig. SM1). After being shaken at room temperature (25.0 ± 0.5 °C) in a tube shaker rotator, the supernatant solutions were analyzed for pH with an Orion glass combined electrode. The tubes were then centrifuged at 9000 rpm for 5 min and the supernatant was separated for phosphate analysis. Because Na–M sample has phosphorous in its structure, blanks containing no phosphate were prepared and analyzed similarly.

In order to evaluate the dissolution of calcite (from calcite–M), and the subsequent precipitation of Ca–P phases in the adsorption experiments, a portion of the supernatant obtained from the blanks and from the experiment after the adsorption of 5 μM (first data point in isotherm curve) and 160 μM (last data point in isotherm curve) of

phosphate was separated for calcium analysis. The concentration of calcium measured after adsorption was then compared with the calcium concentration necessary to produce a saturated solution of HAP ($Ca_5(PO_4)_3(OH)$), Brushite ($CaHPO_4 \cdot 2H_2O$), octacalcium phosphate ($Ca_4H(PO_4)_3 \cdot 3H_2O$), β-calcium phosphate ($Ca_3(PO_4)_2$) and carbonate apatite. The solubility diagram was constructed using the hydrogeochemical code PHREEQC 2.16 (Parkhurst and Appelo, 1999) using the MinteqV4 database.

It is important to note that the aim of the experiments was to reproduce conditions that could occur in natural systems (pH and/or ionic strength changes); therefore the calcite–M suspension was not prepared in order to obtain a pre-equilibrated calcite solution (Sø et al., 2008, 2011). Such experimental conditions could be used to describe the calcite–water interface or to model adsorption experimental data. This is beyond the scope of our study.

2.4. Competitive adsorption experiments

For competition experiments, humic acid (HA) suspensions were prepared from a Fluka humic acid (code: 1415-93-6), which had been previously purified according to the methodology proposed by the International Humic Substances Society (Swift, R.S. 1996). Once the purification was completed, a concentrated stock solution of 2 g L^{-1} was prepared by dissolving a weighted amount of HA at pH 10 during 2 h. The HA stock solution was stored in dark conditions at 5 °C.

The competition experiments were carried out at pH values 4.5 and 7.0. The range of initial concentration of phosphate was the same as previously described and the initial concentration of HA was 100 mg L^{-1}. This value corresponds to the concentration required to produce a high humic acid adsorption onto calcite–M (mean values of isotherm curve — see Fig. SM2). Furthermore, different methods of phosphate and humic acid addition were also considered, i.e.: (i) simultaneous addition of both adsorbates; (ii) phosphate added first and then humic acid; (ii) humic acid added first, and phosphate added second. Between each adsorbate addition, the equilibrium time was 3 h. In each case, the concentration of calcite–M was 1 g L^{-1} and the ionic strength was 0.001 M $NaNO_3$. Once the samples were shaken at the required time, the supernatant solutions were analyzed for pH, centrifuged at 9000 rpm for 5 min and the supernatant was then separated for humic acid and phosphate analysis.

2.5. Raman spectroscopy analysis

In order to discriminate between adsorption and precipitation of Ca–P compounds, Raman spectroscopy was performed. Raman spectroscopy is a powerful, nondestructive tool that can be used to analyze chemical and structural changes at the micrometer scale level (1 μm) which occur on the surface. This technique can also be used to identify different phases present in the material. The spectra were obtained with a LabRam (Horiba/Jobin Yvon) spectrograph equipped with confocal microscope. A small portion of the samples obtained after adsorption of 5 μM and 160 μM of phosphate were placed in glass sample holder and gently pressed. A small portion of the sample was focused with the microscope and then a laser beam (632 nm) was directed onto the sample. The exposure time was 10 s and the accumulation number was 10.

The same procedure was performed with a sample of powder $CaCO_3$ previously adsorbed with phosphate (5 μM), and with the calcite–M sample without adsorbed phosphate. All data collected were baseline-corrected.

2.6. Chemical analysis

Phosphate and HA concentration were measured using a UV–VIS spectrophotometer (Shimadzu UV–VIS 1700) equipped with a 1-cm quartz cell. For phosphate, the method proposed by Murphy and Riley (1962) was used.

The concentration of HA in the solution was measured at 550 nm (Vermeer et al., 1998); the solution samples had previously been buffered (pH ~ 8.7) with 0.05 M $NaHCO_3$ (Iglesias et al., 2010).

The phosphate and humic acid adsorbed were calculated by measuring the difference between the initial and remaining concentrations in the solution.

3. Results and discussion

3.1. Solid characterization

Table SM3 (see supplementary material) shows the chemical compositions of the synthesized solid samples. Both samples have similar Si, Al, Fe, Mn, Mg, K and P contents, according to their predominant mineralogical composition (montmorillonite). The main differences can be seen in the Na and Ca contents. The amount of Ca in the calcite–M sample is 61.5 mg g^{-1}; the amount added during the synthesis was 80 mg g^{-1}. The increase in calcium content corresponds with the decrease in Na content, and results show that in the interlayer ~40% of sodium is displaced by calcium ions. Besides, this increase also leads to an increase in SSA, as measured by N_2 adsorption. Although this method is not recommended to measure the surface area of expandable materials, such as clays, the values obtained indicate that at least the porosity of the material changes after the synthesis, perhaps due to calcite. According to XRD analysis (Fig. 1), calcite is the main solid phase obtained during the synthesis, after the incorporation of calcium. Fig. 1 shows the XRD pattern of Na and calcite–M. The pattern of Na–M is typical of a sodium-exchanged montmorillonite with quartz and perhaps some feldspar impurities (Borgnino et al., 2009). It shows the 001 reflection at 7.8 °2θ, corresponding to a basal spacing, *d*001, of 11.4 Å, which is normal for a sodium montmorillonite (Moore and Hower, 1986). The XRD pattern of calcite–M is very similar to that of Na–M, however the 001 reflection is barely able to be perceived. A limited reflection, hardly perceptible, seems to be present at a lower angle, around 6.8 °2θ, which corresponds to a higher basal space, *d*001 = 13.0 Å (Fig. 1). The poorly defined diffraction 001 reflection could be related to a greater loss of the silicate sheets stacking along the c-direction, which may be associated with a partial exfoliation or delamination of the clay layers (Gilman and Morgan, 2003; Zapata et al., 2013). Taking into account that the descriptions of calcite are usually referred to as a hexagonal cell, with an *a* axis of 0.59 nm and a *c* axis of 1.706 nm (Doner and Warren, 1989), a possible value of *d*001 = 13.0 Å (1.30 nm) could indicate

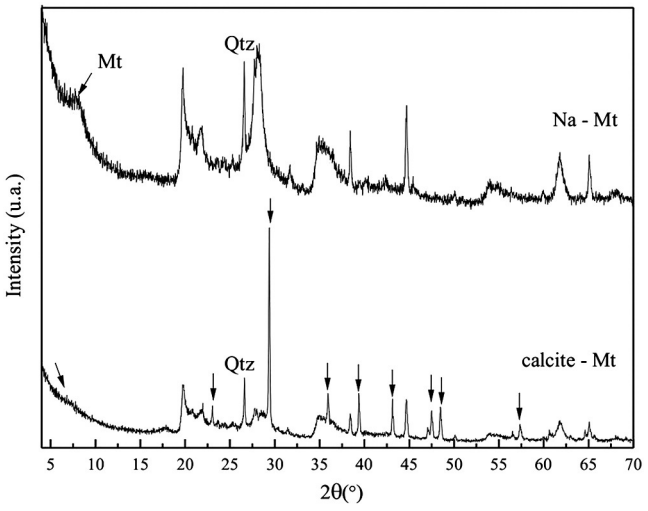

Fig. 1. XRD pattern of Na–M, calcite–M. Reflections assignments are as follows: Mt, montmorillonite; Qtz, quartz; Cal, calcite (arrows).

that the calcite is incorporated into the interlayer space (perhaps distorted) or onto the basal surface, opening and increasing the interlayer space and removing the reflection 001. Additionally, typical reflections of calcite are present in the XRD pattern of calcite–M (Fig. 1). The peak in 29.1 °2θ position is the most intense peak, usually used to identify calcite. Other less intense peaks are located at 43.1, 47.4, 48.5 and 57.4 °2θ. As a result, the chemical composition and XRD pattern demonstrate that the calcium added during synthesis is mainly in basal surfaces or interlayer spaces, such as calcite. Based on this result, it would be expected that the clay only acts as a carrier or support of calcite, and the coating would be the responsible for phosphate adsorption.

Zeta potential measurements were performed to evaluate whether calcite could alter or change the surface net negative charge of montmorillonite (see Fig. SM4). The net negative charge observed in both montmorillonite samples is the result of the presence of structural negative charges within the clay lattice. The positive charge that can be generated at the broken edges of the clay layers at low pH is not enough to produce significant modifications in the zeta potential values as this charge is much lower than the structural charge (Duc et al., 2005 and references therein). Although calcite could contribute with positively charged groups, its presence does not contribute significantly the net charge of the montmorillonite; the zeta potential values of montmorillonite remain negative in the studied pH range.

3.2. Adsorption experiments

3.2.1. Effect of pH on phosphate adsorption

Several factors may cause changes in phosphate adsorption when pH levels are modified. First, changes in pH may produce modifications in the surface net charge of calcite–M in addition to phosphate speciation. Furthermore, the dissolution of calcite or precipitation of Ca–P compounds is also pH dependent. Fig. 2 shows a clear dependence of phosphate adsorption on pH, whereas the adsorption increases with decreasing pH. The same behavior has been observed for the other tested ionic strength conditions evaluated (0.1 and 0.001 M, not shown here). Liu et al. (2012) found similar results, in contrast with the results of Karageorgiou et al. (2007) and Millero et al. (2001) who observed an increase in phosphate adsorption with increasing pH. In the experiments of Karageorgiou et al. (2007), the differences could have been due to the high initial concentration of phosphate used, promoting the precipitation of Ca–P compounds. Millero et al. (2001) performed their experiments in seawater solution. The chemical composition included cations and anions, including HCO_3^-, which may compete with phosphate for adsorption sites. Such competition could explain the decrease in phosphate adsorption when the pH decreased from 8.5 to 7.5. Regarding the shape of the isotherm curve (Fig. 2), two parts can be distinguished: the first can be described approximately by a Langmuir isotherm where a saturation of the adsorption capacity is reached; the second where a continuous increase without a saturation of the surface is observed.

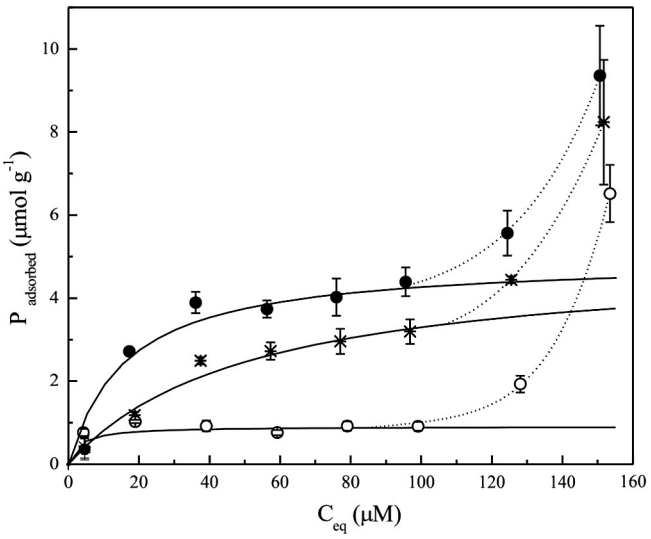

Fig. 2. Phosphate adsorption onto calcite–M. Solid circles: pH 4.5; cross: pH 7.0; open circles: pH 9.0. Lines only serve as guide to eyes. Error bars represent the standard deviation of duplicate sample measurements.

The phosphate adsorption capacity of Na–M is very poor (Borgnino et al., 2009). Considering that montmorillonite only serves as a carrier of calcite and assuming that phosphate is preferentially adsorbed onto calcite sites (Sø et al., 2011), the observed pH dependence is a consequence of both the increase of phosphate protonated species and the concentration of positive surface sites of calcite–M. According to the calcite surface sites concentrations obtained by modeling (see SM5 for details), the >Ca sites are dominated by $>CaOH_2^+$ and $>CaCO_3^-$ with less than 10% of the $>CaHCO_3^0$ site. Given that the phosphate is preferentially adsorbed onto Ca sites> (Sø et al., 2011), the contribution of positive surface sites of calcite ($>CaOH_2^+$) is 2%. Simple calculations may be performed to estimate this percentage. Assuming that this sample is a mix of calcite and Na–M, calcite contributes with 3.04×10^{-4} mol of positive sites g^{-1} (see Fig. SM5a). Therefore, in 1.0615 g of calcite–M mixture containing 0.0615 g of calcite and 1.0 g of Na–M, calcite provides 1.85×10^{-5} mol of positive sites and montmorillonite 9.17×10^{-4} mol of negative sites. These represent 2.0% of positive sites and 98% of negative sites, which may explain the low adsorption capacity of phosphate onto calcite–M system (about 10 times less) in relation to calcite (Yagi and Fukushi, 2012). The low concentration of positive surface sites and the consistently net negative surface charge of calcite–M limit the adsorption of phosphate, even at low pH.

The other factor controlling adsorption is the surface precipitation of Ca–P compounds. The first way to determine whether surface precipitation is occurring is by the shape of the adsorption curve. Adsorption can be explained based on a number of theoretical models; Langmuir and Freundlich models are the most used. For our experimental data, the Langmuir model fits well. It is important to mention here that although the Langmuir model fits the experimental data, this does not imply that the adsorption of phosphate onto calcite–M takes place according to the conditions established by the model. Considering the shape of the isotherm curve obtained in this work, the sole purpose of using the mathematical model is to discriminate between adsorption and surface precipitation. Thus, for data that fit the model, the main process then is adsorption. For those conditions where data do not follow the mathematical model (e.g.: for high values of initial concentration experimental data move away from Langmuir behavior), surface precipitation predominates. Fig. 2 shows that for low-to-moderate initial phosphate concentration, the isotherm shapes are typically L-type. Hence, the decrease in phosphate solution concentration is likely for adsorption process. At higher concentration (>100 μM), the phosphate removal greatly increases and the behavior deviates from L-type. By definition, the surface precipitation is the process by which a solid phase grows on the surface of a particle, as a continuation of a surface complexation process. Once the phosphate was adsorbed, the following increase in phosphate concentration leads to the pre-nucleation and subsequent growth of Ca–P phases onto calcite–M. It was demonstrated that the crystal nucleation starts with the formation of aggregates of calcium phosphate pre-nucleation clusters that densify at a templating phosphate pre-nucleation surface. Then, the densification of the clusters leads to the formation of an amorphous precursor phase, which finally is transformed into a crystalline apatite (Dey et al., 2010; Gebauer et al., 2008). Consequently, the deviation from the Langmuir type observed in our experiments could be explained by the formation of secondary minerals onto the calcite–M surface. This behavior has previously been reported by other authors (Griffin and Jurinak, 1973; Sø et al., 2011). Our experimental results that indicate that surface precipitation occurs under conditions of high phosphate concentrations, however cannot be ruled out entirely for low concentrations, particularly between pH

~7.0 and 9.0, wherein the precipitation of Ca–P compounds (i.e.: HAP) is favored.

3.2.2. Effect of ionic strength on phosphate adsorption

Fig. 3a and b portrays the sorption isotherms for phosphate adsorption onto calcite–M under 0.1 M, 0.01 and 0.001 M $NaNO_3$ solutions at pH values 4.5 and 7.0. The sorption of phosphate decreases with ionic strength at any initial phosphate concentration and pH but, as can be seen from the shape of the adsorption curves, the effect of ionic strength varies. The adsorption data obtained at 0.001 M follow the L-type isotherm adsorption curve, while 0.1 and 0.01 M of $NaNO_3$ do not.

The ionic strength dependency on adsorption is sometimes considered evidence for outer-sphere or inner-sphere coordination. Ions that form outer-sphere complexes compete for adsorption sites with ions of the supporting electrolyte. In this case, a decrease in the adsorption is observed when the electrolyte concentration is increased. Conversely, ions that form inner-sphere complexes are directly coordinated with surface groups and do not compete or compete on a limited scale with electrolyte ions, so adsorption is less affected by a change in the ionic strength (Sparks, 2002). Although the results may indicate outer-sphere complexes, phosphate most likely adsorbs via inner-sphere coordination onto hydr(oxides), (Antelo et al., 2005; Mallet et al., 2013) Fe-exchanged montmorillonites (Borgnino et al., 2009) and also calcite (Sø et al., 2011). Therefore, in this case, the effect of ionic strength could not help to distinguish the type of surface complexes (outer or inner complex) that phosphate forms onto calcite–M.

A possible explanation for the effect of ionic strength may be the changes in the concentration of calcite charged groups, as a result of ionic strength variations (Sø et al., 2011). Calculation with the SCM model modified to give a CCM model (see Fig. SM5b) shows that a small change in the concentration of the calcite charged groups is produced when ionic strength is increased from 0.01 to 0.1 M. The concentration of the negatively charged surface species increases by 2.6% (mainly $>CaCO_3^-$) whereas the concentration of the positively charged species decreases by 2.6% (mainly $>CaOH_2^+$). As a consequence, the overall negative charge density increases and the adsorption decreases. This increase in negatively surface charge groups would represent a decrease of 2.6% in the adsorption capacity. However, the phosphate adsorption at 0.1 M of $NaNO_3$ decreases by 50% in relation to the adsorption capacity at 0.01 M. Therefore, the change in surface concentration may contribute to the decrease in the adsorption of phosphate, but another factor also controls the decrease in phosphate adsorption. One other option is the dissolution of calcite, which is favored at acidic pH values and high ionic strengths. If the calcite is dissolved, not only would less surface sites be available to adsorb phosphate, but also similarly, more calcium in the solution could precipitate as Ca–P compounds. This is expected to occur, especially at 0.1 and 0.01 M of $NaNO_3$ where the adsorption isotherm curves deviate from the Langmuir behavior model (Fig. 3a and b). According to our data, the amount of calcite dissolved at pH values 4.5 and 7.0 in 0.1 M $NaNO_3$ is 6.3% and 3.8% (see Table SM6). In turn, the presence of phosphate in the solution favors the dissolution of calcite. Klasa et al. (2013) found that the dissolution of calcite in the presence of phosphate at high ionic strengths resulted in a higher calcite dissolution rates. Data of calcium concentration obtained at different pH values for experiment made with $P_i = 50$ and 160 μM and at different ionic strengths (see Fig. SM7 and Table SM6) shows that pH, ionic strength and phosphate concentration all affect calcite dissolution. For pH 4.5, high ionic strength and phosphate concentration promote dissolution, as calcium increase in those conditions (Fig. SM7). At pH 7.0 the dependence is less pronounced, and only at 160 μM of P does the calcium concentration change considerably, in this case decreasing with ionic strength (see Table SM6). Calcium concentrations obtained at pH 7.0 are most likely the result of the dissolution of calcite, and subsequent precipitation of Ca–P compounds.

3.2.3. Raman spectroscopy and solubility curve analysis

In order to evaluate the conditions that promote adsorption or surface precipitation, Raman spectroscopy of the calcite–M–P samples obtained after adsorption of phosphate at Pi = 5 μM and 160 μM (pH values 4.5 and 7.0; 0.1 and 0.001 M of $NaNO_3$) was conducted. The spectra obtained were then compared to the Raman spectra of calcite–M and to the spectra of calcite after it had adsorbed 5 μM of phosphate (calcite–P), in the same condition as previously mentioned. The latter spectrum was performed in order to evaluate the main vibration bands, which describe the phosphate adsorbed/precipitated onto calcite. To interpret the results obtained, two analyses were performed concurrently. First, the Raman spectra of phosphate adsorbed samples were compared to the spectra of the phosphate species in solution at the same pH, which were obtained from literature. Second, to discriminate adsorption from surface precipitation, the spectra of calcite–M–P (phosphate adsorbed onto calcite–M sample) samples were compared with Raman spectra of calcium phosphate compounds, which were obtained from literature. In conjunction with this analysis, solubility diagrams of calcium compounds were constructed. The saturation of the solution in calcium for certain Ca–P compounds was analyzed and then compared with the amount of calcium obtained during adsorption experiments.

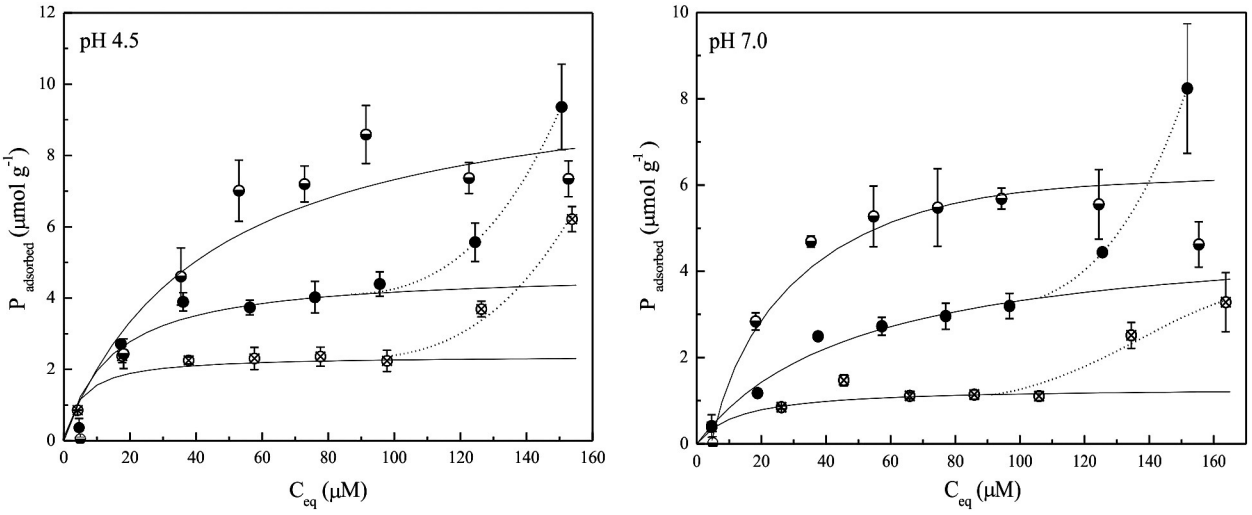

Fig. 3. Effect of ionic strength on phosphate adsorption at: left pH 4.5 and right pH 7.0. Half-open circles: 0.001 M $NaNO_3$; solid circles: 0.01 M $NaNO_3$; cross-circle: 0.1 M $NaNO_3$. Lines only serve as guide to eyes. Error bars represent the standard deviation of duplicate sample measurements.

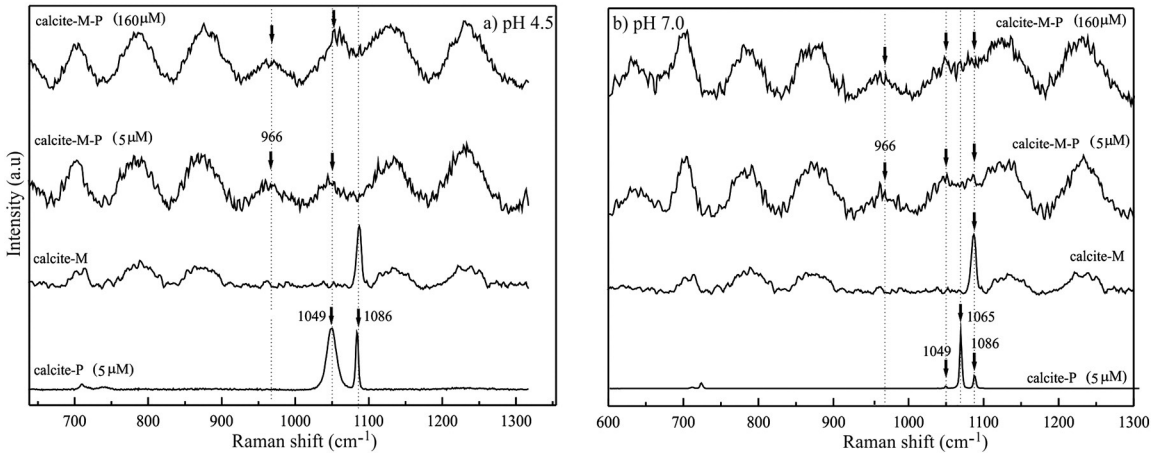

Fig. 4. Raman spectra of calcite–M and calcite after adsorbed phosphate at: a) pH 4.5 and b) pH 7.0. Ionic strength: 0.001 M $NaNO_3$.

Fig. 4a shows the results obtained at pH 4.5 and ionic strength of 0.001 M. The spectra of calcite–P have well defined peaks, typical of crystalline solids, with two intense peaks, one at 1086 cm^{-1} and the other at 1049 cm^{-1}. The first peak corresponds to the υ_1 CO_3 mode and is the most intense in calcite samples. The Raman spectra of calcite–M are typical of amorphous materials, with a low degree of crystallinity and very broad bands. It shows a strong symmetric peak at 1086 cm^{-1} together with a series of bands that may identify the main vibration modes of montmorillonite. According to Bishop and Murad (2004), the Raman bands in the spectral region of 800–600 cm^{-1} are caused by the vibrational modes of Si – O – Si bonds, which connect the SiO_4 tetrahedra that make up a layer. Between the spectral regions of 1150–800 cm^{-1}, the observed bands arise from the stretching mode of the Si – O bond in SiO_4 tetrahedra and for Al_2O_3 in lattice. Turning to the spectrum of calcite–M–P, at this pH and ionic strength the Raman spectrum shows the vibration modes of montmorillonite previously mentioned and two broad bands at 966 cm^{-1} and at 1049 cm^{-1}.

At 1049 cm^{-1}, the strongest band present in calcite–P may be related to a shift of the main bands (1074–1150 cm^{-1}) of the $H_2PO_4^-$ in solution, related to PO_2 stretching vibration band (Preston and Adams, 1979). This same band also appears in the calcite–M–P samples and is more intense for the highest initial phosphate concentration. The band at 966 cm^{-1} could be related to the shift of the 940 cm^{-1} stretching band, which corresponds to the P – $(OH)_2$ stretching bands in $H_2PO_4^-$ aqueous solution (Preston and Adams, 1979). Actually, this band is typically used to identify HAP precipitates, as it is the most intense band in this compound. The solubility diagram curves obtained for this experimental condition are plotted in Fig. 5. Here, the calcium concentration, obtained after adsorption at pH 4.5 and for the two initial phosphate concentrations is below the limit of the HAP solubility (log K_{Hap} −44.3). This suggests that the precipitation of this phase should not take place in these experimental conditions. With this in mind and considering that the band at 1049 cm^{-1} is present either in calcite–P and calcite–M–P, the interpretation of this band under this pH condition could represent the shifts of the PO_2 stretching band, and may indicate the presence of phosphate adsorbed, in an inner-sphere surface complex. The Langmuir type adsorption behavior observed at pH 4.5 and 0.001 M of $NaNO_3$ supports this interpretation. The band at 966 cm^{-1}, could be related to shifts in the P – $(OH)_2$ stretching band, and may also indicate the presence of a phosphate surface complex. These surface complexes may perhaps then act as the initial nuclei for HAP precipitation, when the conditions of precipitation are adequate. However, under these experimental conditions, adsorption prevails in respect to surface precipitation.

At pH 7.0 (Fig. 4b) the results obtained show some similarities with pH 4.5. For calcite–P, the peak at 1086 cm^{-1} is present, but the peak at 1049 cm^{-1} is hardly seen. In addition, a new band appears at 1065 cm^{-1}. This band could be related to the vibrational modes of υ_3 $P0_4$ + $\upsilon_1 CO_3$; it is normally present in carbonate apatites (Antonakos et al., 2007; Zhou, 2011). For calcite–M–P samples, the spectra have two broad bands, one at 966 cm^{-1} and the other at 1049–1080 cm^{-1}. The latter seems to be the resulting contribution of the two bands (1049 cm^{-1} + 1065 cm^{-1}). The interpretation of the 1049 cm^{-1} band is the same as the previously made interpretation. Regarding the band at 1065 cm^{-1}, the solubility diagram shows (Fig. 5) that at pH_i 7.0, for both initial phosphate concentrations, the calcium concentrations obtained after adsorption are above the limit of HAP saturation; even more, they register as above the carbonate apatite saturation limit. Therefore, at pH 7.0 adsorption does occur while some precipitation is also present. The pH conditions favor that precipitation process occurs.

A similar analysis was conducted with the results which were obtained from Raman spectra of the samples, after the adsorption of phosphate at higher ionic strength (0.1 M $NaNO_3$). For pH 4.5 and for calcite–P sample, bands at 1049 and 1065 cm^{-1} are present, indicating that adsorption and some precipitation of a carbonate apatite could be happening (Fig. 6a). Actually, the last band is more intense than the band at 1049 cm^{-1}. These same two bands are present for the calcite–M–P sample (P_i = 5 μM), although the band at 1049 cm^{-1} is hardly visible. Here, the well-defined peak which was obtained may indicate that the analysis was perhaps made over a precipitated phase, as is very different from the other calcite–M spectra. At P_i = 160 μM, the Raman

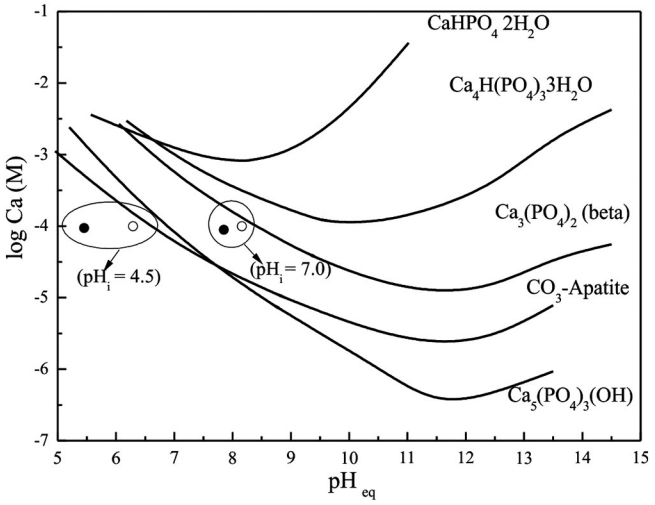

Fig. 5. Solubility diagrams for Ca–P compounds. Solid circles: P_i = 50 μM; open circles: P_i = 160 μM. Ionic strength: 0.001 M $NaNO_3$.

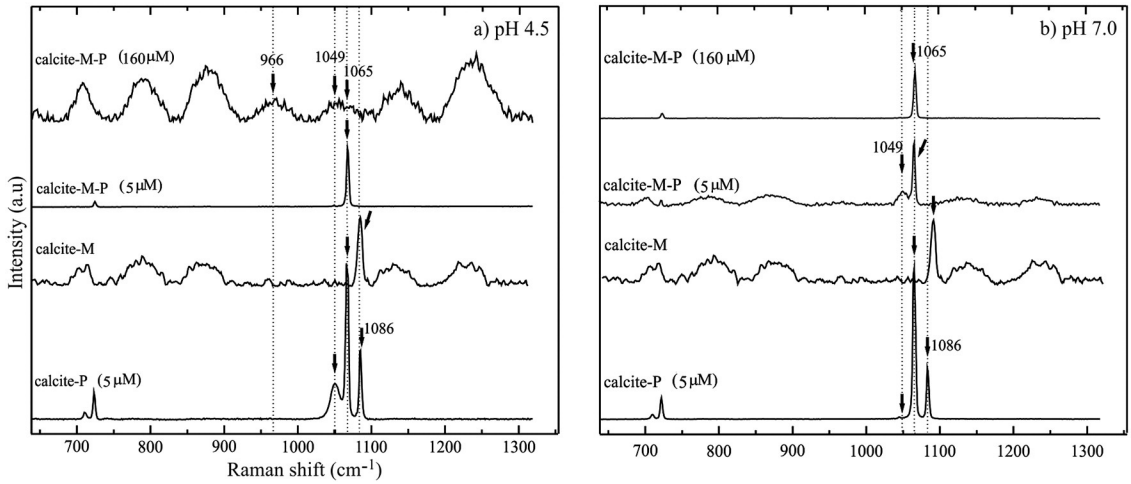

Fig. 6. Raman spectra of calcite–M and calcite after adsorbed phosphate at: a) pH 4.5 and b) pH 7.0. Ionic strength: 0.1 M $NaNO_3$.

spectra shows broad bands, one at 966 cm^{-1} and the other between 1049 and 1065 cm^{-1}. The interpretation of these bands is the same as the one which was made at 0.001 M $NaNO_3$. However, high ionic strength condition also promotes dissolution of calcite (see Fig. SM7) and precipitation of Ca–P compounds. Fig. 7 shows that the calcium concentration measured after adsorption has saturated in carbonate apatite, which confirms that this compound may be present under these conditions. At pH 7.0 (Fig. 6b), the same band (1065 cm^{-1}) is also present in all evaluated phosphate conditions. In fact, the solubility diagram also shows that for either P_i concentration, the calcium concentration is saturated in carbonate apatite. Clearly, high ionic strength, pH and phosphate concentration promote the precipitation of Ca–P compounds; in our experiments as carbonate apatites. The band at 1049 cm^{-1} is also present at $P_i = 5$ μM, which indicates that adsorption also occurs, although precipitation should be the dominant process.

3.2.4. The effect of humic acid on phosphate adsorption: order of addition

Humic acid and phosphate are usually present together in water. The humate ligand, containing carboxyl groups, could compete with phosphate for binding to calcium ions. However, in competition the adsorption behavior may be changed by both the presence of a competitor as well as by the way that the competitor is introduced to the system. Fig. 8a and b shows the effects of humic addition on phosphate adsorption at pH values 4.5 and 7.0, at an initial humic acid concentration of 100 mg L^{-1}. For both pH levels, when both ligands were added simultaneously (together), a reduction on phosphate adsorption was observed. This finding suggests that HA and phosphate could be adsorbed simultaneously at the calcite–M surface, and compete for common surface sites. The reduced proportion on phosphate adsorption was similar for pH values 4.5 and 7.0 (~20%), suggesting that HA adsorbs larger amounts than phosphate onto calcite surface, leaving less surface sites available for the phosphate adsorption, even at pH 4.5, where phosphate adsorbs more. The reduction was greater when humic acid was added first (HA + P) and at pH 4.5, where it is expected that humic acid is absorbed in a larger amount. Humic acid is a negatively charged molecule. The steric effect and the increase of the negative charge at the interface prevent the approximation of phosphate at the surface, and adsorption, therefore, is reduced. Clearly, the phosphate ions cannot displace the humic acid from the surface.

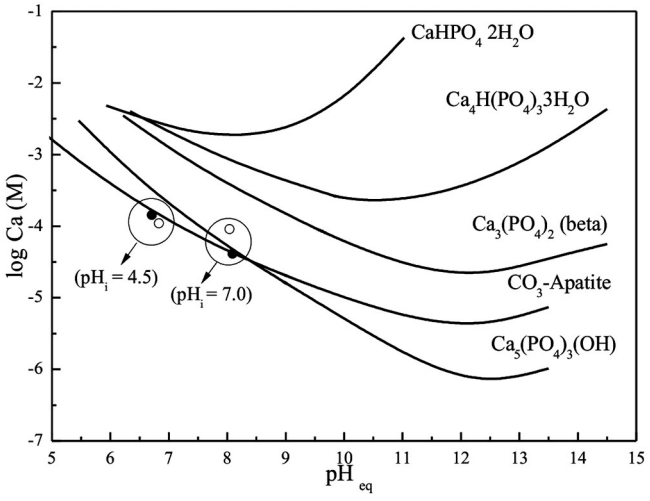

Fig. 7. Solubility diagrams for Ca–P compounds. Solid circles: $P_i = 50$ μM; open circles: $P_i = 160$ μM. Ionic strength: 0.1 M $NaNO_3$.

In contrast to the previously mentioned cases, the phosphate adsorption increases when phosphate is added first (P + HA). In this case, phosphate is adsorbed first and when humic acid is added second, the adsorption also occurs but in a greater amount than without HA. Because HA has a strong affinity for calcium ions, the addition can also influence the saturation state of Ca–P compounds and may explain this behavior. Although precipitation of Ca–P compounds is favored at high ionic strengths, precipitation was also observed with Raman spectroscopy for experiments at 0.001 M $NaNO_3$ (Fig. 4). Perhaps humic acid prevents precipitation and therefore more phosphate ions are available for adsorption. The increase in phosphate adsorption is greater at pH 7.0, where precipitation of Ca-compounds is expected to be higher.

4. Conclusions

As pH and ionic strength decrease, the adsorption of phosphate onto calcite–M increases. However the mechanism by which phosphate is removed is different; it depends on the initial concentration of phosphate. While adsorption is favored for low ionic strength and phosphate concentrations lower than 100 μM, surface precipitation is favored for high phosphate concentration and ionic strength. Because surface precipitation is a continuation of surface complexation, it is expected that adsorption would dominate in the beginning of the process. As phosphate concentration increases, surface precipitation starts, producing Ca–P compounds, mainly carbonate apatite. The transition between adsorption and surface precipitation and the identification of the Ca–P compound formed have been shown by Raman spectroscopy. Changes in ionic strength also influence the phosphate sorption, decreasing as ionic strength increases. This effect can be accounted for an increase in

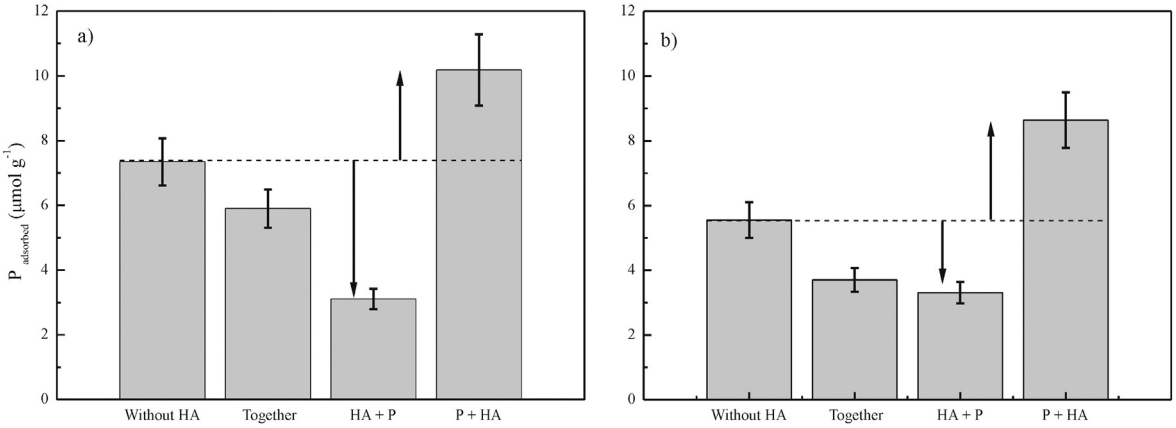

Fig. 8. Effect of the order of addition of the adsorbates on phosphate adsorption: a) pH 4.5 and b) pH 7.0. The values plotted correspond to Γ_{max} adsorption values for phosphate adsorption in the absence and in the presence of humic acid.

the concentration of negative surface sites, as well as an increase in the calcite dissolution, which promotes the formation of Ca–P compounds.

The experimental competition results clearly show that while competition between humic acid and phosphate does occur, the order of addition strongly affects the phosphate adsorption. When HA and phosphate are added simultaneously, or HA is added first, the phosphate adsorption decreases. When phosphate is introduced first, an increase in the phosphate adsorption is recorded, perhaps due to inhibition produced by the HA in the precipitation of Ca–P compounds.

Acknowledgments

The authors wish to acknowledge the assistance of the Consejo Nacional de Investigaciones Científicas y Tecnológicas (CONICET) and the Universidad Nacional de Córdoba, both of which support facilities used in this investigation. This work was financed by Argentina's SECYT-UNC (2011-2012) and CONICET. L. Borgnino, is a member of CICyT in Argentina's CONICET (2012-2014). Language assistance by native English speaker Wendy Walker is gratefully acknowledged.

Appendix A. Supplementary data

Supplementary data to this article can be found online at http://dx.doi.org/10.1016/j.geoderma.2014.06.017.

References

Alvarez, R., Evansa, L.A., Milhamb, P.J., Wilson, M.A., 2004. Effects of humic material on the precipitation of calcium phosphate. Geoderma 118, 245–260.
Antelo, J., Avena, M., Fiol, S., Lo'pez, R., Arce, F., 2005. Effects of pH and ionic strength on the adsorption of phosphate and arsenate at the goethite–water interface. J. Colloid Interface Sci. 285, 476–486.
Antonakos, A., Liarokapis, E., Leventouri, T., 2007. Micro-Raman and FTIR studies of synthetic and natural apatites. Biomaterials 28, 3043–3054.
Bishop, J.L., Murad, E., 2004. Characterization of minerals and biogeochemical markers on Mars: a Raman and IR spectroscopic study of montmorillonite. J. Raman Spectrosc. 35, 480–486.
Borgnino, L., Avena, M.J., De Pauli, C.P., 2009. Synthesis and characterization of Fe(III)-montmorillonites for phosphate adsorption. Colloids Surf. A 341, 46–52.
Castro, B., Torrent, J., 1995. Phosphate availability in calcareous vertisols and inceptisols in relation to fertilizer type and soil properties. Fertil. Res. 40, 109–119.
Cole, C.V., Olsen, S.R., Scott, C.O., 1953. The nature of phosphate sorption by calcium carbonate. Soil Sci. Soc. Am. Proc. 1953 (17), 352–356.
Delgado, A., Madrid, A., Kassem, S., Andreu, L., Campillo, M., 2000. Phosphorus forms and desorption patterns in heavily fertilized calcareous and limed soils. Soil Sci. Soc. Am. J. 64, 2031–2037.
Delgado, A., Madrid, A., Kassem, S., Andreu, L., Campillo, M., 2002. Phosphorus fertilizer recovery from calcareous soils amended with humic and fulvic acids. Plant Soil 245, 277–286.
Dey, A., Bomans, P.H.H., Müller, F.A., Will, J., Frederik, P.M., de With, G., Sommerdijk, N.A.J. M., 2010. The role of prenucleation clusters in surface-induced calcium phosphate crystallization. Nat. Mater. 9, 1010–1014.
Doner, H.E., Warren, C.L., 1989. Carbonate, halide, sulfate, and sulfite minerals. In: Dixon, J. B., Weed, S.D. (Eds.), Minerals in Soils Environments. Soil Science Society of America, Madison, Wisconsin, pp. 279–330.
Duc, M., Gaboriaud, F., Thomas, F., 2005. Sensitivity of the acid–base properties of clays to the methods of preparation and measurement 1. Literature review. J. Colloid Interface Sci. 289, 139–147.
Freeman, J.S., Rowell, D.L., 1981. The adsorption and precipitation of phosphate onto calcite. J. Soil Sci. 32, 75–84.
Gebauer, D., Viilkel, A., Ciilfen, H., 2008. Stable prenucleation calcium carbonate clusters. Science 322, 1819–1822.
Gilman, J.W., Morgan, A.B.J., 2003. Characterization of polymer-layered silicate (clay) nanocomposites by transmission electron microscopy and X-ray diffraction: a comparative study. Appl. Polym. Sci. 87, 1329–1338.
Griffin, R.A., Jurinak, J.J., 1973. The interaction of phosphate with calcite. Soil Sci. Soc. Am. J. 37, 847–850.
Grossl, P.R., Inskeep, W.P., 1991. Precipitation of dicalcium phosphate dihydrate in the presence of organic acids. Soil Sci. Soc. Am. J. 55, 670–675.
House, W.A., Donaldson, L., 1986. Adsorption and coprecipitation of phosphate on calcite. J. Colloid Interface Sci. 112, 309–324.
Iglesias, A., López, R., Gondar, D., Antelo, J., Fiol, S., Arce, F., 2010. Adsorption of MCPA on goethite and humic acid-coated goethite. Chemosphere 78, 1403–1408.
Inskeep, W.P., Silvertooth, J.C., 1988. Inhibition of hydroxyapatite precipitation in the presence of fulvic, humic, and tannic acids. Soil Sci. Soc. Am. J. 52, 941–946.
Karageorgiou, K., Paschalis, M., Anastassakis, G.N., 2007. Removal of phosphate species from solution by adsorption onto calcite used as natural adsorbent. J. Hazard. Mater. 139, 447–452.
Klasa, J., Ruiz-Agudo, E., Wang, L.-J., Putnis, C.V., Valsami-Jones, E., Menneken, M., Putnis, A., 2013. An atomic force microscopy study of the dissolution of calcite in the presence of phosphate ions. 117, 115–128.
Klelner, J., 1988. Coprecipitation of phosphate with calcite in lake water: a laboratory experiment modelling phosphorus removal with calcite in Lake Constance. Water Res. 22, 1259–1265.
Liu, Y., Sheng, X., Dong, Y., Ma, Y., 2012. Removal of high-concentration phosphate by calcite: effect of sulfate and pH. Desalination 289, 66–71.
Mallet, M., Barthélémy, K., Ruby, C., Renard, A., Naille, S., 2013. Investigation of phosphate adsorption onto ferrihydrite by X-ray photoelectron spectroscopy. J. Colloid Interface Sci. 407, 95–101.
Millero, F., Huang, F., Zhu, X., Liu, X., Zhang, J.-Z., 2001. Adsorption and desorption of phosphate on calcite and aragonite in seawater. Aquat. Geochem. 7, 33–56.
Moore, D.M., Hower, J., 1986. Ordered interstratification of dehydrated and hydrated Na-smectite. Clay Clay Miner. 34, 379–384.
Murphy, J., Riley, J.P., 1962. A modified single solution method for the determination of phosphate in natural waters. Anal. Chim. Acta. 27, 31–36.
Oelkers, E.H., Golubev, S.V., Pokrovsky, O.S., Benezeth, P., 2011. Do organic ligands affect calcite dissolution rates? Geochim. Cosmochim. Acta 75, 1799–1813.
Parkhurst, D.L., Appelo, C.A.J., 1999. User's guide to PHREEQC (version 2). A computer program for speciation, bath reaction, one-dimensional transport and inverse geochemical calculations. Water Resources Investigations Report 99-4259. U.S. Geological Survey, Denver, Colorado.
Peinemann, N., Ferreiro, E.A., Helmy, A.K., 1972. Estudio mineralógico de una montmorillonita de Cerro Bandera (Provincia de Neuquén, República Argentina). Rev. Asoc. Geol. Argent. 27, 399–410.
Preston, C., Adams, W.A., 1979. A laser Raman spectroscopic study of aqueous orthophosphate salts. J. Phys. Chem. 83, 814–821.
Sample, E.C., Soper, R.J., Racz, G.J., 1980. Reactions of phosphate fertilizers in soils. In: Khassawneh, F.E., Sample, E.C., Kamprath, E.J. (Eds.), The Role of Phosphorus in Agriculture. ASA, CSSA, SSSA, Madison, WI, pp. 263–310.
Sø, H.U., Postma, D., Jakobsen, R., Larsen, F., 2008. Sorption and desorption of arsenate and arsenite on calcite. Geochim. Cosmochim. Acta 72, 5871–5884.
Sø, H.U., Postma, D., Jakobsen, R., Larsen, F., 2011. Sorption of phosphate onto calcite; results from batch experiments and surface complexation modeling. Geochim. Cosmochim. Acta 75, 2911–2923.

Sparks, D.L., 2002. Environmental Soil Chemistry. Academic Press, San Diego Madison, WI, pp. 1018–1020.
Staunton, S., Leprince, F., 1996. Effect of pH and some organic anions on the solubility of soil phosphate: implications for P bioavailability. Eur. J. Soil Sci. 47, 231–239.
Stumm, W., Leckie, J.O., 1970. Phosphate exchange with sediments: its role in the productivity of surface water. Advances in Water Pollution Research, vol. 2. Pergamon Press, pp. 26/1–26/16 (Part III).
Vermeer, A.W.P., Van Riemsdijk, W.H., Koopal, L.K., 1998. Adsorption of humic acid to mineral particles. 1: specific and electrostatic interactions. Langmuir 14, 2810–2819.
Violante, A., Gianfreda, L., 1993. Competition in adsorption between phosphate and oxalate on an aluminum hydroxide montmorillonite complex. Soil Sci. Soc. Am. J. 57, 1235–1241.
Wandruszka, R.V., 2006. Phosphorus retention in calcareous soils and the effect of organic matter on its mobility. Geochem. Trans. 76, 6.
Yagi, S., Fukushi, K., 2012. Removal of phosphate from solution by adsorption and precipitation of calcium phosphate onto monohydrocalcite. J. Colloid Interface Sci. 384, 128–136.
Yin, H., Yun, Y., Zhang, Y., Fan, C., 2011. Phosphate removal from wastewaters by a naturally occurring, calcium-rich sepiolite. J. Hazard. Mater. 198, 362–369.
Zapata, P.A., Belver, C., Quijada, R., Aranda, P., Ruiz-Hitzky, E., 2013. Silica/clay organo-heterostructures to promote polyethylene–clay nanocomposites by in situ polymerization. Appl. Catal. A 453, 142–150.
Zhou, D., 2011. An in-vitro model of calcium phosphate mineralization in bone: transformation from amorphous calcium phosphate to apaptite. (Thesis (M.S.)) Central Michigan University.